

THESIS FOR THE DEGREE OF LICENTIATE OF ENGINEERING

## Evaluation of Capillary Flow in Gels

The Liquid Uptake of Capillaries and Gelation Mechanisms in Alginate Gels

JOHANNA ANDERSSON

Department of Chemistry and Chemical Engineering

CHALMERS UNIVERSITY OF TECHNOLOGY

Gothenburg, Sweden 2016

Evaluation of Capillary Flow in Gels  
The Liquid Uptake of Capillaries and Gelation Mechanisms in Alginate Gels  
JOHANNA ANDERSSON

© JOHANNA ANDERSSON, 2016.

Licuppsatser vid Institutionen för kemi och kemiteknik  
Serie Nr: 2016:11  
ISSN: 1652-943X

Department of Chemistry and Chemical Engineering  
Chalmers University of Technology  
SE-412 96 Gothenburg  
Sweden  
Telephone + 46 (0)31-772 1000

Cover:

From left to right: example of capillary flow with stained water flowing upwards a channel in an alginate gel; a stained cell solution has penetrated a capillary alginate gel, page 22; series of micrographs with water penetrating a capillary in an alginate gel coming from the left side, page 28.

Printed by Chalmers Reproservice  
Gothenburg, Sweden 2016

# Evaluation of Capillary Flow in Gels

## The Liquid Uptake of Capillaries and Gelation Mechanisms in Alginic Gels

JOHANNA ANDERSSON

Department of Chemistry and Chemical Engineering

Chalmers University of Technology

### ABSTRACT

For centuries it has been known that wetting liquids penetrate porous materials if the pores are sufficiently small. In some cases the liquid penetration is desired, like in kitchen paper or diapers, in other systems the penetration should be minimised or avoided, like in water repellent textiles or paper printing. Either way capillary flow has been studied extensively starting from smooth to rough surfaces and from single capillaries to porous systems. However, one field, which is lacking attention is the behaviour of capillary flow in porous gels. How does a semi-solid material influence capillary flow? Possible applications could be to absorb solutes or cell solutions in porous gels with the aim to get an even distribution of those. In this thesis alginic and agarose gels are used to study capillary flow. A thorough study of the gel characteristics including rheology measurements and investigation of the microstructure using two different gelation mechanisms gave the basis to study capillary action in air filled capillaries in alginic gels. A fast method to create a single capillary of tailored diameter in an alginic gel as well as in agarose gel was developed. Pure water penetrated the 5–6 cm long horizontal channel in an alginic gel of 630 µm, containing predominantly water in just 0.8 seconds. With that I showed first (i), that it is possible to get spontaneous capillary flow in gels containing large amounts of water and second (ii), I showed that the penetration dynamics follow the expected behaviour in that the squared travelled distance is proportional to the time,  $x^2 \propto t$ . As anticipated smaller capillaries exhibit slower uptake and higher viscosities decrease the speed in addition, as tested with a sucrose and a hydroxyethyl cellulose solution. Yet, the predictions from Lucas and Washburn theory optimised for hard systems, like glass result in times of only 0.2 seconds for water in a diameter of 630 µm and 5 cm length compared to the experimentally determined value of 0.8 seconds. Also all other tested liquids and diameters result in slower speeds than predicted for tested alginic and agarose gels. The most common reasons to address discrepancies to the prediction like inertial forces and using the dynamic contact angle instead of static, fail to explain the observed discrepancy, as I will show in this thesis. Other reasons are given and analysed. Since the spreading speed of a liquid drop on a soft surface has shown to be decreased and a wetting ridge at the three-phase contact line has been observed, it is hypothesised that the capillary flow is slowed down by such a wetting ridge, occurring in the front of the moving meniscus in the capillary. Besides the known viscous energy dissipation in the liquid, a viscoelastic energy dissipation due to the wall has to be added, which is the object of further investigations.

Keywords: Capillary flow, capillary action, alginic gel.

# LIST OF PUBLICATIONS

This thesis is based on the following papers, referred to by the Roman numerals in the text. The papers are appended at the end of the thesis.

- I. Microstructural, mechanical and mass transport properties of isotropic and capillary alginate gels**  
Erich Schuster, Johanna Eckardt, Anne-Marie Hermansson, Anette Larsson, Niklas Lorén, Annika Altskär, and Anna Ström  
*Soft Matter* **10**, (2014) 357–66
- II. Unpredicted capillary filling dynamics in semi-solid channels**  
Johanna Andersson (former Eckardt), Anna Ström and Anette Larsson  
*Manuscript*

Papers not included in this thesis

- i. Long-term frozen storage of wheat bread and dough – effect of time, temperature and fibre on sensory quality, microstructure and state of water**  
Johanna Eckardt, Camilla Öhgren, Ayse Alp, Susanne Ekman, Annika Åström, Guo Chen, Jan Swenson, Daniel Johansson, and Maud Langton  
*Journal of Cereal Science* **57**, (2013) 125–33

# CONTRIBUTION REPORT

- I.** Responsible for writing parts of the manuscript and analysis of the results with the co-authors as well as the fabrication of alginate gels and solutions.
- II.** Responsible for writing, planning the experiments and conducting the experiments under supervision and scientific input of the co-authors.

## ABBREVIATIONS

GDL	D-(+)-Gluconic acid $\delta$ -lactone
HEC	Hydroxyethyl cellulose
LW	Lucas Washburn equation
TEM	Transmission Electron Microscopy

# NOMENCLATURE

$\gamma$	Surface Tension (without indices referring to liquid-air)
$\eta$	Viscosity
$\theta$	Contact angle
$\kappa^{-1}$	Capillary Length
$\rho$	Density
$\sigma$	Cutoff length
$\Delta$	Fraction of energy dissipated
$\Phi_S$	Fraction of solid parts
$A$	Area
$\dot{E}$	Energy
$F$	Force
$g$	Gravity on earth
$G$	Elastic (shear) modulus
$h$	Height
$P_A$	Atmospheric pressure
$P_c$	Laplace or capillary pressure
$P_e$	External pressure
$r$	Roughness factor
$R$	Radius
$S$	Spreading coefficient
$t$	Time
$U$	Speed
$x$	Travelled distance of a meniscus

# CONTENTS

<b>1</b>	<b>Introduction</b>	<b>1</b>
<b>2</b>	<b>Background</b>	<b>3</b>
2.1	Surface tension and wetting . . . . .	3
2.1.1	Surface tension . . . . .	3
2.1.2	Wetting . . . . .	5
2.1.3	Measuring techniques for surface tension and contact angle . . . . .	9
2.2	Capillary action in single capillaries . . . . .	11
2.2.1	Lucas-Washburn (LW) model . . . . .	12
2.2.2	Modifications of LW . . . . .	13
2.3	Polysaccharide gels . . . . .	13
2.3.1	Mechanical and mass transport properties . . . . .	14
2.3.2	Alginate . . . . .	14
2.3.3	Agarose . . . . .	16
2.4	Rheology of viscoelastic polymers . . . . .	17
<b>3</b>	<b>Experimental</b>	<b>19</b>
3.1	Alginate gels . . . . .	20
3.2	Agarose gels . . . . .	21
<b>4</b>	<b>Results and discussion</b>	<b>22</b>
4.1	Capillary alginate gels . . . . .	22
4.2	Alginate gels produced <i>via</i> internal vs. external gelation . . . . .	23
4.2.1	Mechanical properties depend on gelation mechanism . . . . .	23
4.2.2	Microstructural differences . . . . .	24
4.3	Liquid penetration into air filled capillaries in hydrogels . . . . .	25

4.3.1	Possible reasons for the deviation of experiment and LW . . . . .	27
<b>5</b>	<b>Conclusion and future work</b>	<b>30</b>
5.1	Conclusion . . . . .	30
5.2	Future work . . . . .	31



# CHAPTER 1

## INTRODUCTION

Capillary flow or spontaneous uptake of liquids in porous systems is of outstanding relevance from an industrial point of view. The fields of application range wide, from pharmaceutical applications, such as disintegration of tablets and powder technology over textile processing to drying of mortar and paint and even oil recovery. The porous materials and their characteristics are equally widespread as the industrial applications in terms of pore geometry, chemical composition and rheology. Extensive research has been carried out over many centuries to characterise liquid flow and in the end to be able to tailor mass transport to desired values.

Capillary action is flow driven by surface forces of the material and the imbibing liquid, without the application of an external pressure. The height a liquid travels in a single capillary, also referred to as *Jurin's height*, was described by James Jurin (1684- 1750) [1]. About two centuries later Lucas [2] and Washburn [3] described capillary flow in porous systems seen as a bundle of straight capillaries of uniform radius of a certain inclination. Today in 2016, many questions have been answered already. Capillary flow in single capillaries has been described horizontally as well as vertically [2–5], capillary flow in porous systems has been modelled and characterised with different models and approaches [2, 3, 5]. Roughness of the channel walls has been introduced and the flow was characterised [6–8] and capillary sizes of micrometre [9–13] and even nanometre sizes [14–16] have been studied for capillary flow experimentally. One field which currently is being studied is wetting on soft surfaces where the elastic modulus of the material influences the spreading behaviour of a liquid drop [17–19]. As wetting is related to capillary flow, it is assumed that the rheological behaviour of a solid also influences the

spontaneous liquid uptake in these systems [20].

An example of such soft surfaces can be gels, for instance alginate gels. Alginate is a polysaccharide derived from seaweed and is popular for its availability and its biocompatibility. In food products it is often used as thickening agent but it also finds use as a matrix for cell growth, preferably in capillaries in micrometer range [21–24]. Agarose is another biocompatible and widely used polysaccharide, which forms a gel upon cooling after being heated. One way of introducing a cell solution or solutes in a porous gel is to pump the solution into the gel. However, there are several disadvantages accompanied with this method, one being unevenly dispersed cells [21]. An easier mechanism could be to use capillary flow to distribute cells in a capillary system of a gel matrix, which has been done on dried alginate gels [25], but the drying step can even be removed as I show in this thesis. Despite extensive research, it was not part of investigations to study capillary flow in capillaries of soft gel systems, even though it is fundamental to understand the mechanism to optimise cell seeding or similar systems where capillary action occurs in gels.

In this study I show that capillary inflow occurs with pure water and other liquids in capillaries created in gels, even though they contain 98 % water itself. Alginate gel can be produced in such a way that it forms circular straight capillaries of tailored diameters [26]. Finding the right model system for investigating the rheologic behaviour and the microstructure of a capillary alginate gel was studied. The capillaries in the gel were produced by introducing cross-linking ions via an external source as well as producing gels via an internal route where the resulting gel did not exhibit any capillaries. I investigated the spontaneous uptake of liquids in circular capillaries of alginate and agarose gels. Liquids with different viscosity, activities and surface tension were used, namely pure water, a sucrose solution (21.4 % w/w) and a hydroxyethyl cellulose (HEC) solution (0.1 % w/w) in capillaries of 180 to 630  $\mu\text{m}$  in diameter. The results are compared to the existing models for hard systems of Lucas and Washburn.

# CHAPTER 2

## BACKGROUND

This chapter describes the state of the art in surface phenomena and material characterisation necessary to understand and interpret the experiments and results in this thesis.

### 2.1 SURFACE TENSION AND WETTING

All materials have a surface energy which is decisive for their behaviour in contact with other materials. When a drop of water is deposited on a smooth and clean glass surface, it will spread to a rather flat drop exhibiting a small contact angle with the glass. A water droplet on a plastic or on teflon will maintain a high contact angle, which is due to the surface energy of the material. The mechanism behind builds the basic of capillary flow and is described in the two sections below, 2.1.1 and 2.1.2. Methods of measuring the contact angle and surface tension are explained in section 2.1.3.

#### 2.1.1 SURFACE TENSION

The surface tension of liquids, often denoted with  $\gamma$  or sometimes  $\sigma$ , can cause a water droplet to maintain its shape on a hydrophobic surface, it is for example the reason why foam in a bathtub can occur. Whenever one phase meets another, an interfacial tension becomes apparent, which is equivalent to its surface energy [27]. It is visible by the behaviour of the phases, usually the liquid phase in that a water droplet for example forms a large or small contact angle in contact with a hard substrate. The liquid phase usually has the tendency to maintain the smallest possible surface (typically a sphere).

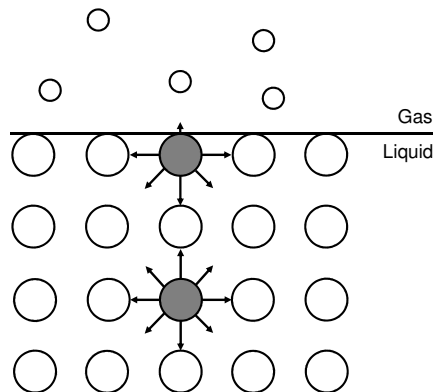


**Figure 2.1:** Schematic drawing explaining surface tension from a molecular perspective. The molecule at the interface is more drawn towards the bulk because it is less attracted by the gas molecules. The net force is downwards.

The physical reason for that is depicted in Fig. 2.1. A molecule in the bulk is surrounded by a number of other molecules to which it is in contact through intermolecular attractive interactions [1, 27], which could for example be van der Waals forces or the much stronger hydrogen bonds. As water molecules have relatively strong intermolecular forces, water has a very high surface tension (72 mN/m for pure water at 25 °C) compared to many other substances. A molecule in the bulk has the same amount of forces in each direction. A molecule exposed to another phase, for example air, has an imbalance, since the attractive force to air molecules is less. The net force therefore makes the molecule to be drawn towards the bulk of the liquid, which implies that the surface is maintained as small as possible in contact to air. The surface tension is therefore a measure of the strength of cohesive forces, *i.e.* the forces *inside* a medium, but also taking into account the adhesive forces, *i.e.* the interaction with another medium, such as air. The opposing force is often gravity, which can prevent droplets from exhibiting perfectly spherical shapes. The threshold above which gravitational forces become predominant can be quantified by the capillary length described in section 2.1.3. Surface tension is the reason why a water strider can hold itself on the water surface without drowning. If a washing-up liquid is added, it would sink because the liquid contains surfactants, which are surface active agents. They decrease the surface tension by aligning themselves on the water-air interface having their polar head in water and their non-polar tail in air [27]. Fig. 2.2 illustrates the influence of

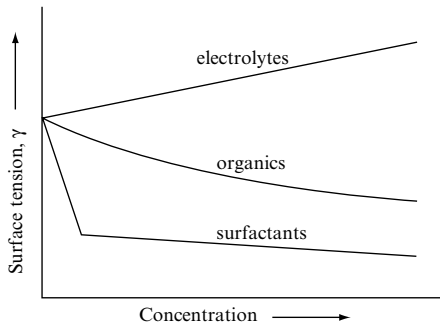


**Figure 2.2:** Influence of added components on the surface tension  $\gamma$  to an aqueous system. With permission from [27].

surfactants, organics and electrolytes on  $\gamma$  in aqueous systems. Surfactants decrease the surface tension drastically until all surfaces are covered where the critical micelle concentration (CMC) is reached, after which  $\gamma$  is practically constant [27]. Higher concentrations result in an increasing amount of micelles inside the bulk, which does not contribute to decrease the surface tension. Organics, such as ethanol, normally decrease the surface tension with increasing concentration [27]. They prefer to absorb at the liquid-air surface. This is a time dependent process, thus, the surface tension can be dynamic within a certain time frame. If  $\gamma$  of a water-ethanol solution is measured, it will decrease over time until the equilibrium value is reached, which is lower than the arithmetic mean between the two pure component surface tensions [27]. This is due to that the component with the lower surface tension, ethanol in this case, will preferentially be located at the surface. The dynamic surface tension is important when the liquid does not have enough time to equilibrate, for example in capillary action or printing processes [27].

### 2.1.2 WETTING

Wetting describes how a liquid deposited on a solid or liquid spreads [1]. For a drop on a solid surface, the contact angle  $\theta$  can be determined, which characterises wetting. Fig. 2.3(a–c) depicts the shapes a drop can adopt on a solid surface. If the liquid spreads completely on the surface and forms a liquid film, the contact angle is zero, this case is referred to as *complete wetting*, see Fig. 2.3(a). When  $0^\circ < \theta < 90^\circ$  partial wetting occurs (Fig. 2.3(b)) and if  $\theta > 90^\circ$  the liquid does not wet the surface (Fig. 2.3(c)) [1]. If the contact angle

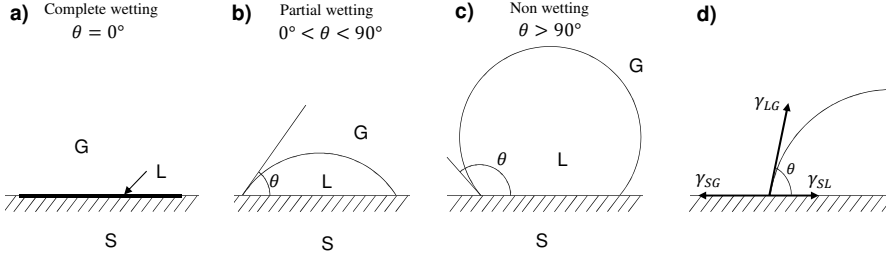


**Figure 2.3:** A drop on a surface can deposit different shapes depending on the surface tension of all the three phases, liquid, solid and gas. (a) A droplet is complete wetting,  $\theta = 0^\circ$ , (b) partial wetting when  $0^\circ < \theta < 90^\circ$ , (c) the drop is non wetting when  $\theta > 90^\circ$ , (d) illustrates the forces acting on the three-phase contact line.

is very large, usually above  $120^\circ$ , the surface is referred to as superhydrophobic, which will be explained below. These kind of surfaces are usually textured where the liquid does not penetrate small gaps in between obstacles and forms a high contact angle due to the air pockets created in these gaps. Wetting is closely related to the surface tension which is described above in section 2.1.1. The relation of forces at equilibrium at the three-phase contact line is depicted in Fig. 2.3(d) and characterised by Young's equation:

$$\gamma_{SG} = \gamma_{SL} + \gamma_{LG} \cos \theta \quad (2.1)$$

where the subscripts  $S, L$  and  $G$  stand for the solid, liquid and gas phase respectively. With that the surface tension can be directly linked to the contact angle. Just like the surface tension, the contact angle is often time dependent. A drop deposited on a surface can spread from partial wetting (Fig. 2.3(b)) to complete wetting (Fig. 2.3(a)) in a certain time frame. Spreading is characterised by the spreading coefficient  $S$ , which is defined as [27]:

$$S = \gamma_{SG} - \gamma_{SL} - \gamma_{LG} \quad (2.2)$$

Spreading occurs as long as  $S > 0$  [27].

**TEXTURED SURFACES** On smooth hydrophobic surfaces the maximum contact angle can reach around  $\gamma = 120^\circ$  [28, 29]. However, a rough hydrophobic surface can exhibit much higher contact angles up to almost  $180^\circ$  [30] where the liquid forms a nearly perfectly spherical shape on a surface. Wenzel [31] introduced a roughness factor  $r$  defined as the ratio between the true surface

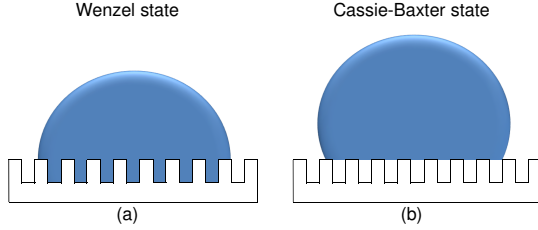


**Figure 2.4:** A water droplet sunk into the structure representing the Wenzel state (a) and repelled by the structure showing the Cassie-Baxter state (b)

area compared to the apparent one (also termed *Wenzel roughness*):

$$\cos \theta^* = r \cos \theta \quad (2.3)$$

where  $\theta$  is the Young contact angle on a smooth surface and  $\theta^*$  is the real measured or apparent contact angle. On perfectly smooth surfaces  $r = 1$  and for rough surfaces  $r > 1$ . For contact angles on smooth surfaces smaller than  $90^\circ$ , meaning that  $\cos \theta < 1$ , the resulting contact angle  $\theta^*$  for rough surfaces becomes smaller, and the substrate appears more hydrophilic. On the other hand, if the initial contact angle on smooth surfaces is larger than  $90^\circ$  and a roughness on the surface is introduced will result in that the surface becomes even more hydrophobic. However, the Wenzel roughness is not an absolute measurable value, it can only be used as a comparison between surfaces. Moreover, roughness can sometimes be observed at different length scales, which is nano- and microroughness, including features intrinsic to production processes [32]. They are fluctuations in the surface of short wavelengths, but they are large compared to molecular dimensions. Macroroughness or waviness are surface irregularities of longer wavelengths [32]. The latter usually does not influence the contact angle. In many cases of rough hydrophobic surfaces Eq. (2.3) does not hold and droplets exhibit a substantially larger contact angle than predicted. That is due to trapped air in cavities of roughness, see Fig. 2.4(b).

In nature this phenomenon can be seen for instance on the leafs of the plant *Lotus* or on *Salvinia* [33]. When their leafs are submerged into water air pockets remain on the surface of the leafs, which is observed by a silvery shine. The phenomenon was described by Cassie and Baxter [34], who extended the theory of Wenzel, depicted in Fig. 2.4(a–b). The Wenzel state (Fig. 2.4(a)) refers to a droplet on a structured surface filling the gaps if the surface is hydrophilic enough and if the geometry of the patterns allow it [35]. In the

Cassie-Baxter state (or Fakir state, Fig. 2.4(b)) the droplet does not touch the bottom of the structured surface leaving air pockets below. A droplet rolling off the surface takes up dust, spores or bacteria and is therefore an optimised protection for plants or the basis for self cleaning surfaces [33]. According to Cassie and Baxter [34]

$$\cos \theta^* = f_1 \cos \theta - f_2 \quad (2.4)$$

where [34, 36]

$$f_1 = \frac{\text{area in contact with liquid}}{\text{projected area}} \quad f_2 = \frac{\text{area in contact with air}}{\text{projected area}} \quad (2.5)$$

If there is no trapped air,  $f_1$  is equal to the Wenzel roughness  $r$  and  $f_2$  becomes zero, then the equation becomes Eq. (2.3). The smaller the contact with the solid parts the higher the resulting contact angle. In that way it is possible to fabricate superhydrophobic surfaces, which are self cleaning and easy to maintain. However, the challenges for large industrial production are still either high production costs or lacking robustness of such surfaces (Joël De Coninck, personal communication, March 16, 2016).

**SOFT SURFACES** When a drop is placed on a rigid surface it spreads until it reaches its thermodynamic equilibrium. Is it placed on a soft solid, the substrate undergoes a local deformation predominantly at the three phase contact line, called a *wetting ridge* [17, 19, 37]. In liquid-impermeable soft substrates the deformation solely originates from the vertical component of the surface tension force, see  $\gamma_{LG}$  in Fig. 2.3(d) [38]. Forced wetting of a water droplet on polydimethylsiloxane through a needle attached to the droplet has been studied recently [17, 18, 37]. First a local deformation is created (see Fig. 2.5(a)) at the contact line which is accompanied by pinning until a certain contact angle is reached after which depinning occurs where the contact line suddenly surfs down the wetting ridge. The phenomenon is termed *stick-slip motion*. The size of the wetting ridge is dependent on the rheology of the substrate [18] and governs the spreading of drops on viscoelastic substrates [17]. On purely elastic solids the work done on the wetting ridge is restored immediately after passage of the moving liquid front as the solid relaxed, no net work is done and no energy is dissipated [19]. On purely viscous solids all energy would be dissipated. But since most semi-solids are viscoelastic a fraction, of the energy expended will be dissipated [19]. Earlier work of Carré et al. [39] shows that the spreading of a drop is substantially slowed down on soft substrates compared to rigid surfaces, see Fig. 2.5(b). For example a nanoscale wetting ridge can slow down the spreading time by more than one

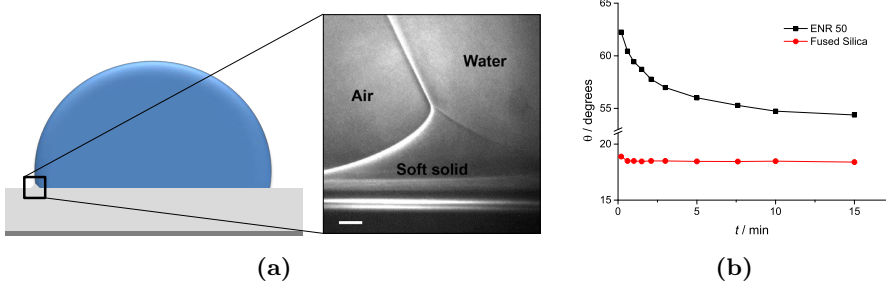


**Figure 2.5:** (a) High-resolution X-ray image of a water droplet deforming a soft substrate, the scale bar is 2  $\mu\text{m}$ , middle image with permission from [18]. (b) Example of the evolution of the dynamic contact angle on a rigid substrate (fused silica, ●) compared to a soft substrate (epoxidised natural rubber, ENR 50, ■) over time, adapted with permission from [39]. On silica the equilibrium contact angle was attained after 20 s compared with ENR, which stabilised after 1 h (at 53°).

order of magnitude [39]. The quantity of energy dissipated is given by [20, 39]:

$$\dot{E}\Delta \approx \frac{\gamma^2 U \Delta}{2\pi G \sigma} \quad (2.6)$$

where  $U$  is the speed at which the triple line moves,  $G$  is the elastic (shear) modulus and  $\sigma$  is a cutoff length below which the solid no longer behaves in a linearly elastic manner (which is typically in the range of a few nanometres for elastomers [40])[19]. Park et al. [18] visualised wetting ridges with transmission X-ray microscopy and found that the cusp of the wetting ridge is bent, see Fig. 2.5(a), while earlier studies, for example of Shanahan and Carre [19] assumed a straight cusp.

### 2.1.3 MEASURING TECHNIQUES FOR SURFACE TENSION AND CONTACT ANGLE

Since surface tension and the contact angle are dynamic processes, upon measuring, care should be taken of which time frame to measure which is relevant to the process. In very fast processes, like it is often in industrial printing, there is no time for a polymer solution to equilibrate. Likewise, the contact angle or surface tension should be measured within the relevant times, see Table 2.1.

Common methods to measure surface tension or contact angle with are

**Table 2.1:** Measuring techniques of surface tension and their corresponding time scales (from [41, p. 1027] and Reinhard Miller, personal communication, March 15, 2016)

Method	Typical available time range
Maximum bubble pressure	0.1 ms – 100 s
Growing drop or bubble	0.01 s – 600 s
Drop volume	0.1 s – 1000 s
Transient drop or bubble relaxation	1 s – 300 s
Plate tensiometry	1 s – 1 year
Pendent drop	5 s – 24 h
Static drop volume	10 s – 1000 s
Sessile drop	10 s – 24 h
Ring tensiometry	1 min – 1 year
Oscillating bubble	0.01 Hz – 500 Hz
Oscillating drop	0.01 Hz – 10 Hz

Plate tensiometry or Wilhelmy plate method, where the downward pull of the liquid on a plate is measured, which is similar to the ring method where the same force is measured removing a ring from a liquid surface [27]. In the fastest method listed here, the maximum bubble pressure method, air is continuously blown through two capillaries, of different diameters, which are placed in the liquid. The pressure required to form a bubble is directly proportional to surface tension of the liquid [27]. The contact angle is most commonly determined by placing a liquid drop on a planar surface (sessile drop) and with the help of a microscopic lens determine the contact angle directly or with the same objective determine a gas bubble adhering at a solid-liquid interface [27]. Care has to be taken that the drop is not too big so that gravitational forces are not dominating. The capillary length  $\kappa^{-1}$  is the length beyond which gravity becomes important and is estimated by setting the Laplace pressure  $\gamma/\kappa^{-1}$  in relation to the hydrostatic pressure  $\rho g \kappa^{-1}$  at a depth  $\kappa^{-1}$  in a liquid, where  $\rho$  is the density and  $g$  the gravity on earth [1]:

$$\kappa^{-1} = \sqrt{\gamma/\rho g} \quad (2.7)$$

For pure water at 20°C the capillary length is 2.7 mm. Determining a contact angle of water with a drop means therefore that the drop should be considerably smaller than 2.7 mm. In a tube having a diameter smaller than the capillary length, capillary action is the main force occurring during imbibition.

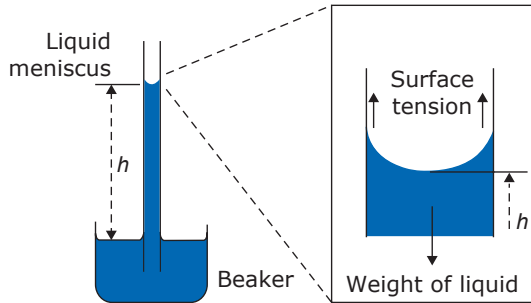


**Figure 2.6:** Capillary rise in a single vertical capillary.

## 2.2 CAPILLARY ACTION IN SINGLE CAPILLARIES

If a thin glass tube is connected to a water reservoir the liquid spontaneously penetrates the tube. This happens typically with decreasing speed over time. The precondition is that the liquid wets the surface (see Fig. 2.3). From an energy point of view, the wet surface has to have a smaller energy than the dry surface,  $\gamma_{SL} < \gamma_{SG}$ , where  $\gamma_{SL}$  and  $\gamma_{SG}$  is the surface tension of the solid-liquid and solid-gas interface, respectively [1]. The relation of the surface energy to the contact angle is described in Young's equation (Eq. (2.1) in section 2.1). Thus, if the contact angle of the liquid on the solid is smaller than  $90^\circ$ , capillary action occurs. This also explains that it is not possible to get capillary action in superhydrophobic surfaces, because the contact angle is larger than  $90^\circ$ , so the liquid does not wet the surface. A wetting liquid forms a concave meniscus inside the capillary (see Fig. 2.6) where the capillary pressure  $P_c$  directly below the meniscus is described using the Laplace equation for spherical interfaces and where the meniscus exhibits a contact angle  $\theta$  with the capillary wall [1, 28]:

$$P_c = P_A - \frac{2\gamma \cos \theta}{R} \quad (2.8)$$

where  $P_A$  is the outer (atmospheric) pressure. If a vertical capillary is considered, the liquid travels up to the height, where the capillary pressure, is equal to the hydrostatic pressure

$$P_A - P_c = \rho g h \quad (2.9)$$

which gives [28]:

$$h = \frac{2\gamma \cos \theta}{R \rho g} \quad (2.10)$$

where  $h$  denotes the height of the meniscus, also referred to as *Jurin's Height*, and  $g$  the acceleration due to gravity. In this way it is possible to determine either the final height of a meniscus or on the other hand if the height is known the equilibrium contact angle or surface tension can be calculated. However, since the equation is missing the time, no information can be obtained about the speed of the liquid while it travels through the capillary. This is achieved by the Lucas-Washburn equation (LW) described in the following section.

### 2.2.1 LUCAS-WASHBURN (LW) MODEL

Independently Lucas [2] and Washburn [3] developed a model, which is now extensively used and referred to as Lucas-Washburn (LW) equation or just Washburn equation. It describes the changing speed of the meniscus over time in a capillary in a porous material. The capillary force  $F_c$  from the curved meniscus is opposed by the force from gravity  $F_h$ , the force from Poiseuille flow  $F_P$  (neglecting air resistance) and inertia  $F_i$  [42]:

$$F_c = F_h + F_P + F_i \quad (2.11)$$

and since  $F = P \cdot A$  it gives:

$$2\gamma \cos(\theta)\pi R = \rho gh(t)\pi R^2 + 8\pi\eta h(t)\frac{\partial h(t)}{\partial t} + \pi R^2 \rho \frac{\partial}{\partial t} \left( h \frac{\partial h(t)}{\partial t} \right) \quad (2.12)$$

where  $\eta$  is the viscosity of the liquid. If a horizontal capillary is considered (renaming  $h$  to  $x$ ) and disregarding inertial forces, which only occur in the very beginning, by integration we receive the typical and simple form:

$$x^2 = \frac{\gamma R \cos \theta}{2\eta} \cdot t \quad (2.13)$$

where  $x$  is the travelled distance and is proportional to the square root of time  $x \propto \sqrt{t}$  or  $x^2 \propto t$ . The contact angle  $\theta$  is assumed to be static and in the Poiseuille flow there is a flow profile of a parabolic shape, where the speed is highest in the middle of the capillary and zero at the wall [43]. Lucas and Washburn aimed to describe liquid in a porous system with a mean capillary radius. In that way the material of capillary transport is described as an idealised bundle of straight pores of uniform diameters. In this study, however, I will focus on the dynamics in single horizontal and straight capillaries of uniform radius.

### 2.2.2 MODIFICATIONS OF LW

LW equation is widely used, but has some assumptions which causes mispredictions or uncertainties in some cases. One example is a porous material with varying pore sizes. In a big pore the liquid accelerates in speed while it decreases the speed in smaller pores. Inertia becomes apparent every time a mass changes its state of motion, like the change of speed. The speed is, thus, constantly changing and hence, inertial forces are not only predominant in the beginning, rather than throughout the system while capillary action occurs [44]. Bosanquet [4] has described inertial flow starting from Eq. (2.12) considering also an external pressure  $P_e$  and letting:

$$\frac{8\eta}{R^2\rho} = a, \quad \frac{P_e R + 2\gamma \cos \theta}{R\rho} = b \quad (2.14)$$

he receives

$$x_2^2 - x_1^2 = \frac{2b}{a} \left\{ t - \frac{1}{a} (1 - e^{-at}) \right\}. \quad (2.15)$$

If  $a \cdot t \ll 1$  and  $P_e = 0$  Eq. (2.15) becomes [44]:

$$x^2 = \frac{2\gamma \cos \theta t^2}{R\rho} \quad (2.16)$$

which describes flow in the inertial regime. The travelled distance  $x$  is directly proportional to the time  $t$ . Higher density leads to slower speeds, while in later times, when viscous forces are predominant, there is no dependency on the density (see Eq. (2.13)).

### 2.3 POLYSACCHARIDE GELS

Polysaccharide gels usually consist of water insoluble polymers of biological origin, composed of the polymer itself which is capable of holding multiple times its own weight of water. In the recent years they are extensively studied due to their fundamental biocompatibility and with it their use in regenerative medicine but also to control drug and protein delivery to tissues and cultures or the use as a scaffold to supply integrity to tissue [45]. In this work polymeric gels of biological origin are used, namely alginate and agarose. In the following a short introduction will be given on general properties of polymeric gels and the two biopolymers alginate and agarose will be described.

### 2.3.1 MECHANICAL AND MASS TRANSPORT PROPERTIES

Generally gels can be divided into two gelling mechanisms, one group are referred to as *physical* and the other ones are *chemical* gels [45–47]. While chemical gels are cross-linked via covalent bonds, physical gels are noncovalent cross-linked gels, formed for example via entanglements, ionic or hydrophobic forces [47, 48]. Unlike covalent bonds in chemical gels, in physical gels the number and position of cross-links can vary with time and temperature [47].

**DIFFUSION** In regenerative medicine a critical characteristic for polymeric gels is their ability to transport or deliver solutes within the bulk network. In most cases diffusion is regarded as the driving transport phenomenon, if there are no large micropores or forced flow in the gel [45]. Considering a component *A* diffusing through component *B* Fick's first law of diffusion can be applied if *P* and *T* are constant:

$$J_{A,x} = -D_{AB} \left( \frac{\partial C_A}{\partial x} \right)_{P,T} \quad (2.17)$$

where  $J_{A,x}$  is the flux in the *x* direction,  $D_{AB}$  is the diffusion constant of *A* diffusing through *B* and  $\partial C_A / \partial x$  is the concentration gradient in the *x* direction. Diffusion alone is, however, slow and not enough to transport nutrients or cells in a gel.

### 2.3.2 ALGINATE

Alginate is an abundant polysaccharide derived from marine brown algae (*Phaeophyceae*) and is also produced by soil bacteria [49]. It is used by the food industry as thickening agent but also in pharmaceutical applications and technical uses as well as biotechnological applications [49]. Alginate is a negatively charged polysaccharide consisting of units of linearly (1→4)-linked  $\beta$ -D-mannuronic acid (M-units) and  $\alpha$ -L-guluronic acid (G-units) [50], see Fig. 2.7. The units tend to arrange in blocks interspersed with regions of alternating structure but showing no regular repeating unit [49]. The composition of M- and G-units depends, besides others, on the plant species, season and growth conditions [50]. During the production process alginic acid is extracted, usually converted to sodium alginate in several steps and finally dried and milled [49]. In the presence of multivalent cations, typically  $\text{Ca}^{2+}$ , alginate forms a gel linking solely the G-units in the gel. The stoichiometric ratio is the ratio between cross-linking units in the gel and multivalent ions and is used to

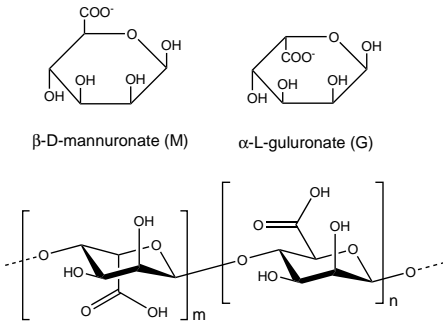


**Figure 2.7:** Alginate consisting of (1-4) linked  $\beta$ -D-mannuronate (M) and  $\alpha$ -L-guluronate (G) monomers which are covalently linked as shown below in different sequences or blocks.

determine the cross-link density and therefore the strength of the gel [51–53]. The network formed is commonly explained by the egg-box-model [50, 54] where the divalent cation links two alginate chains. Since the gelation happens very rapid, simple mixing of an alginate solution with the cation source leads to lumps. Therefore there are commonly two ways to introduce the ions, hereafter called, the *external* and the *internal gelation method*.

**EXTERNAL GELATION METHOD** In the external gelation method the ion source slowly diffuses into the alginate solution, typically through a membrane, see also Fig. 3.2 in section 3.1. By adding the cation source (with an excess of ions compared to G-units) a gel is slowly formed when the ions diffuse into the sol/gel. Straight capillaries with diameters ranging from 50–500  $\mu\text{m}$  are created if alginate is anchored to the wall [55]. The amount and size of the capillaries depends on the type of ion used and the conditions of gelation [56]. In Paper I the external gelation method is used and the microstructure is analysed using transmission electron microscopy (TEM), diffusion measurements and rheology tests and is compared to gels produced by internal gelation.

**INTERNAL GELATION METHOD** Using the internal gelation method an inactive cross-linking ion source, for example calcium carbonate, is mixed into the alginate solution together with a slowly hydrolysing lactone, generally D-(+)-gluconic acid  $\delta$ -lactone (GDL) [49, 57]. Through the acidic properties the calcium is released and a gel is formed. This method is used in Paper II to produce one single alginate capillary in which the dynamics of capillary flow

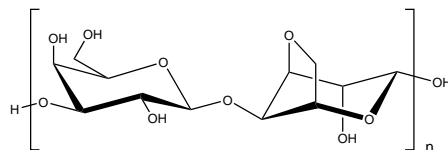


**Figure 2.8:** Main structure of agarose, the neutral fraction of agar containing D-galactose and 3,6 anhydro-L-galactose and attributed primarily to the gel strength in agars.

is determined. The method is also used in Paper I to determine mechanical differences to externally set gels.

**GEL STRENGTH** The strength and elasticity of the gel is dependent on the amount of G-units in the polymer and the distribution of those, which tend to form strong and brittle gels, while more M-units in the polymer chain result in softer and more elastic gels [49]. In addition the average length of G-units correlates with the gel strength [50], indicating that the G-block has to be long enough in order to form a load-bearing junction.

### 2.3.3 AGAROSE

Likewise alginate, agarose is extracted from marine algae, more precisely from various species of red seaweed. It belongs to the class of galactan polysaccharides and forms one of the fractions in agars [58]. Unlike other fractions in agar, agarose is a neutral polymer consisting mainly of linear chains D-galactose and 3,6 anhydro-L-galactose with low sulfate content, see Fig. 2.8 [59]. Agarose is soluble at higher temperatures (at  $\sim 85^\circ\text{C}$ ) and forms a gel upon cooling at 10–40°C, with a gel strength depending on the cooling conditions [58–60]. It is popular for its use in electrophoresis [61], but also clinical diagnostic testing, molecular biology, and biomedical research [58]. Due to the costly extraction process it is only used as a thickener in food applications in form of agar [58]. While in solution agarose chains form random coils, however, upon cooling and in the gel double-helices are present [62] and gelation of agarose is said to be governed by hydrogen bonding [63].

## 2.4 RHEOLOGY OF VISCOELASTIC POLYMERS

If a fluid is in between two parallel plates and the upper one moves forward, shear stress  $\tau$  is the driving force necessary to move the plate per area unit

$$\tau = F/A \quad [N/m^2 = Pa] \quad (2.18)$$

The shear rate  $\dot{\gamma}$  is the rate of deformation when the plates are apart from each other with a gap height  $h$

$$\dot{\gamma} = U/h \quad [s^{-1}] \quad (2.19)$$

and the velocity  $U$  at which the upper plate moves. The shear viscosity  $\eta$  of the liquid is the ratio of shear stress and shear rate

$$\eta = \tau / \dot{\gamma} \quad [Pa \cdot s] \quad (2.20)$$

A Newtonian liquid has the same shear viscosity independent of shear rate, liquids that behave differently are all referred to as non-newtonian. One example of a non-newtonian fluid is a shear thinning liquid. If the viscosity reduces with higher shear rates, the fluid is referred to as shear thinning, also called pseudo-plastic. And conversely if the fluid thickens with higher shear rates, the fluid is referred to as shear thickening or dilatent. Most polymer solutions and melts are non-newtonian liquids, predominantly they are shear thinning due to their long polymer chains [64, 65].

Measuring the stress relaxation involves static measurements, where the stress response of a material is measured to an imposed strain as shown in Fig. 2.9, where (a) shows the applied strain, which is constant after it has reached the desired value and (b) shows the typical stress response for a viscoelastic material. An elastic material, which completely returns to its original shape has a constant stress response irrespective of time, while the stress response of a liquid goes down to zero.

Semi-solid gels are typically characterised dynamically with oscillatory measurements, where for example a cone-and-plate apparatus is used. The measurement gives information about the portion of the elastic and the viscous part, where a certain strain is applied and the stress response is measured. If the material is completely elastic, like a spring, it develops stresses in response to strain that are in-phase with the strain [65]. For a Newtonian fluid (completely viscous) there would be a  $90^\circ$  phase difference between stress and strain and polymer solutions which are partly viscous and partly elastic, so-called viscoelastic fluids, exhibit a phase shift of  $0 \leq \psi \leq 90^\circ$  [65]. The elastic

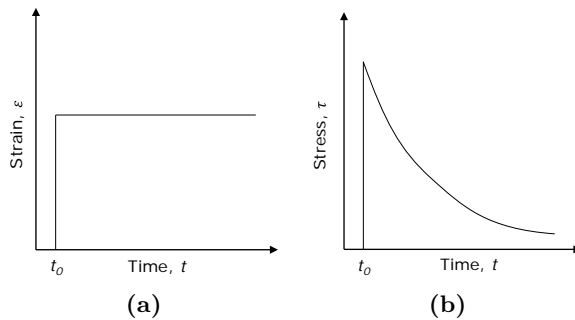


**Figure 2.9:** (a) Applied strain and (b) stress relaxation curve for a viscoelastic material.

and viscous part are commonly described by the storage modulus  $G'$  and the loss modulus  $G''$  respectively, which are defined as

$$G'(\omega) = \frac{\text{in-phase stress}}{\text{maximum strain}} \quad G''(\omega) = \frac{\text{out-of-phase stress}}{\text{maximum strain}} \quad (2.21)$$

where  $\omega$  usually ranges from 0.01 to 500 rad/s [65].

## CHAPTER 3

## EXPERIMENTAL

All experiments carried out in this thesis are based on polysaccharide gels, predominantly on Ca-alginate gels, but also agarose gels. Alginate gels can be prepared in such a way that it spontaneously forms straight circular capillaries of tailored size (for the method description see section 3.1). To find the right gel for a model system for studying capillary flow in, a study on Ca-alginate gels has been carried out investigating the gels of two different gelation methods, internal and external gelation. The focus was put on the differences in microstructure, which was characterised by diffusion and rheology measurements as well as microscopic investigation through transmission electron microscopy (TEM). The outcome of those measurements are described in detail in Paper I and summarised in section 4.2. However, to track the meniscus of a wetting liquid it is difficult just focussing on one of the numerous capillaries in the capillary alginate gel, therefore these gels turned out to be unsuitable for this purpose. A new method has been implemented to conduct and also to measure capillary action in polymeric gels. It is based on creating a capillary having a circular cross-section of sub-millimetre size in the gel. In this way artificial capillaries have been formed using a straight-forward and easy to conduct method, where the channel size can be tailored and with which it was possible to track the wetting liquid over several centimetres in a single capillary in Ca-alginate gels (section 3.1) as well as in agarose gels (section 3.2).

To follow the liquid the flow was videotaped and the video was cut into single images to track the meniscus by using the software ImageJ. In that way the travelled distance over time could be visualised. The results are described in Paper II and summarised and compared to the existing models

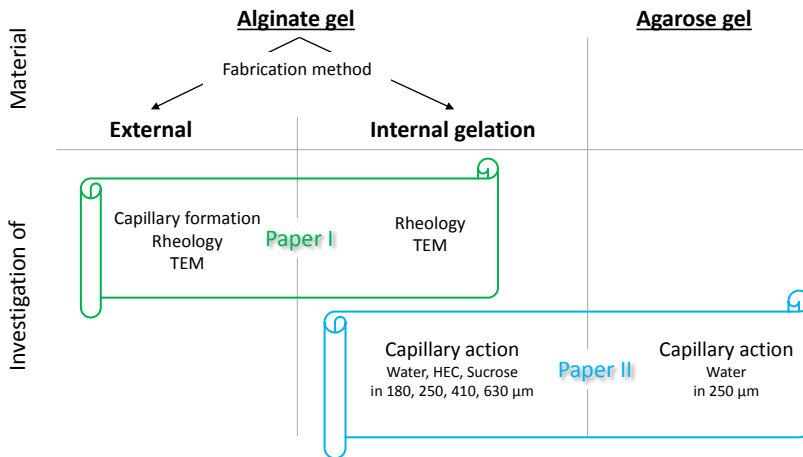


**Figure 3.1:** Outline of the experimental design included in this thesis and the respective papers.

in section 4.3. An overview of the experimental design is schematically given in Fig. 3.1.

### 3.1 ALGINATE GELS

External gelation was conducted as illustrated in Fig. 3.2. A glass beaker was coated with an alginate solution and dried in an oven, which was repeated three times. The alginate solution of 1.8 % was poured into the beaker and by spraying a 0.5 M  $\text{CaCl}_2$  solution on the surface of the solution, a membrane was created. The  $\text{CaCl}_2$  solution was gently poured onto the membrane and allowed to diffuse into the solution. The stoichiometric ratio of cross-linking units to calcium ions was varied from equal amounts to large excess of calcium ions by changing the volume of the 0.5 M solution of  $\text{CaCl}_2$  on top of the alginate solution, see a more detailed description of the method in Paper I. Internal gelation, as it is described in section 2.3.2 has been conducted in Paper I. Likewise the stoichiometric ratio of of calcium ions to G-units was varied, but to a lower extend due to difficulties obtaining a homogeneous gel with large excess of calcium ions. The resulting gels of the two fabrication methods were compared with large deformation.

Moreover, internal gelation has been used to produce one single straight

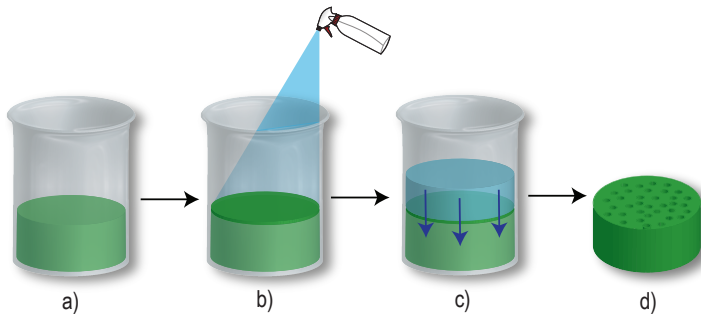


**Figure 3.2:** Creation of alginate capillary gels using external gelation: (a) Liquid sodium alginate solution, (b) spraying of a Ca-solution on the surface to create a gel membrane, (c) adding of the Ca-solution on top of the membrane, so the ions diffuse into the sol/gel, (d) alginate capillary gel after cutting off the top membrane.

capillary of  $\sim 6$  cm length. The gel for wicking experiments was prepared by adding  $\text{CaCO}_3$ , GDL and water to a previously prepared alginate solution (2 %, w/w) and subsequently siphoning the liquid in a 1 ml disposable syringe containing a plastic string. This string formed the capillary and was gently removed directly before the measurement. By changing the thickness of the string, the channel size could be tailored. Before measuring capillary flow the tip of the syringe was cut off and the gel was connected to a liquid droplet. The uptake of the liquid was recorded by a camera (Casio EX-ZR300, Japan) with up to 120 frames per second. The resulting video was cut into single frames with the software FFmpeg (2013-07-09 git-00b1401) and tracking of the liquid was done using ImageJ (1.50b).

## 3.2 AGAROSE GELS

Agarose gels were used to conduct the same wicking tests. Water and agarose was blended and boiled for 5 minutes and the evaporated water was replaced. Likewise the alginate gel, the agarose solution was immediately siphoned in a 1 ml disposable syringe containing a plastic string and cooled at ambient temperature. An agarose concentration of 2 % was used. After 24 h the string was removed and capillary flow was recorded using water as the wetting liquid.

## CHAPTER 4

# RESULTS AND DISCUSSION

This chapter summarises the results of this thesis and discusses possible reasons and hypotheses of the received outcome.

### 4.1 CAPILLARY ALGINATE GELS

An alginate solution results in a capillary gel using a method as described before. The capillaries are homogeneously distributed and by increasing the amount of calcium ions, the diameter of the capillaries can be decreased [66], Paper I. Figure 4.1(a–b) shows two micrographs of capillary gels of which (a) shows a cross-sectional slice of a Ca-alginate gel illustrating the distribution and size of capillaries and (b) shows a freeze-dried alginate gel, which is cut in the direction of the capillaries. It can be seen that the capillaries are straight vertical pores, which are evenly distributed. Note that the process of freeze-drying made the gel walls thinner than they were in a wet gel. Fig. 4.1(c) illustrates a piece of a capillary gel, which has been put on a cell solution to demonstrate that the solution is spontaneously being taken up by the capillaries with capillary flow and, thus, suggesting a possible use for cell seeding. In Paper I capillary diameters ranging from 60 to 110  $\mu\text{m}$  where obtained. If a cross-linking ratio of < 2 of calcium ions to G-units is used, no capillaries were formed, showing that an access of  $\text{Ca}^{2+}$  ions are necessary to form capillaries [57], Paper I. The density of capillaries increased consistently by increasing the ionic strength of the solution on top of the gel.

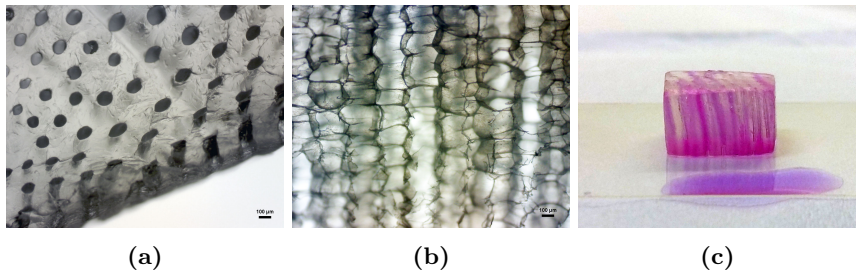


**Figure 4.1:** Capillary alginate gels prepared *via* external gelation, where (a) shows a micrograph of a slice of the gel and (b) shows a micrograph of the freeze-dried gel in a section cut in capillary direction and (c) shows a stained cell solution being taken up by the capillaries in a gel of 50 mm height. The scale bars are 100 µm in (a) and (b).

## 4.2 ALGINATE GELS PRODUCED *via* INTERNAL VS. EXTERNAL GELATION

Calcium-alginate gels produced by internal and external gelation method are characterised. Hereafter a description of the rheological behaviour is given and the micrographs taken with TEM are described and differences discussed.

### 4.2.1 MECHANICAL PROPERTIES DEPEND ON GELATION MECHANISM

Rheological measurements were done by uniaxial compression of the two types of gels while having the same stoichiometric ratio and an alginate concentration of 2 %. The shear stress to maintain the gel at various deformations was measured and is plotted in Fig. 4.2(a) for 5 % and 4.2(b) for 10 % strain. Characteristic for physically cross-linked polymer gels, the stress response at a given deformation decays exponentially, as seen in the figure. This behaviour was observed for both gelation mechanisms and all strains tested, and is a typical viscoelastic behaviour. The stress levelled off to a nearly constant non-zero value in the case of internally set alginate gels. At a given strain less pressure was required to maintain the externally set gel compared to the internally set gel. The Young's modulus, at times also termed elastic modulus, was determined to 11 kPa for internal gels. It will be of importance in section 4.3, where capillary flow in internal gels is discussed. Fig. 4.2(c)

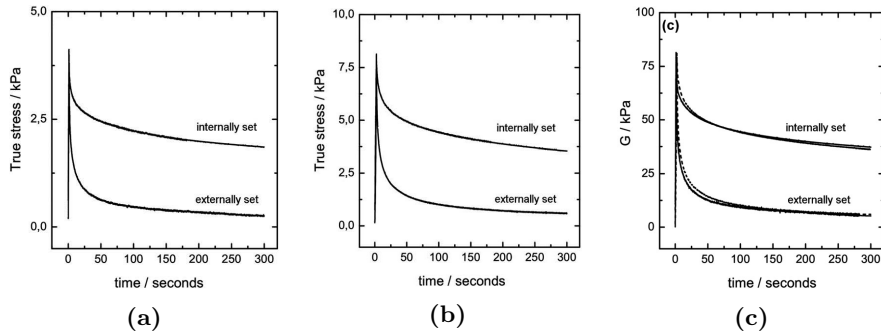


**Figure 4.2:** Stress relaxation curves at (a) 5 % strain and (b) 10 % strain and (c) modulus  $G$  for 5 % strain (solid line) and 10 % strain (dashed line) for internal and external gelation (Paper I).

shows the modulus  $G$  ( $G$  = stress/strain) with 5 % strain (solid line) and 10 % strain (dashed line) over time for internally and externally set gels. A clear difference of internally gels having considerably higher  $G$ -values can also be observed here. The modulus  $G$  is related to Young's modulus, the latter being of importance for wetting properties of the gels [17, 19] and will be discussed more for the experiments on capillary flow described in section 4.3.

When recovering from deformation, externally set gels showed higher plasticity in that the gel did not return to its initial shape as much as internally set gels did (see Table 1 in Paper I). The dependence of stress and strain is, moreover, different for the two gels (Fig. 4.2(c)). The large discrepancy suggests that the methodology of gelation introduces deviations also in the microstructure of the gel, *i.e.* it is not only the macroscopic difference, the presence of the capillaries, causing the difference in mechanical/rheological properties of the gel.

#### 4.2.2 MICROSTRUCTURAL DIFFERENCES

Images of the microstructure with slices of 60 nm were taken using TEM and are depicted in Fig. 4.3(a–b), where (a) shows an internally set and (b) externally set gel. Voids of about 50 nm and above can be observed for both types of gels, similar to pore sizes of carrageenan and pectin [67, 68]. As alginate gels belong to the category of physical gels and with that rather inhomogeneous gels, a wide range of pore sizes can be observed. The largest size is about 200 nm, but also dense network clusters are visible. Between

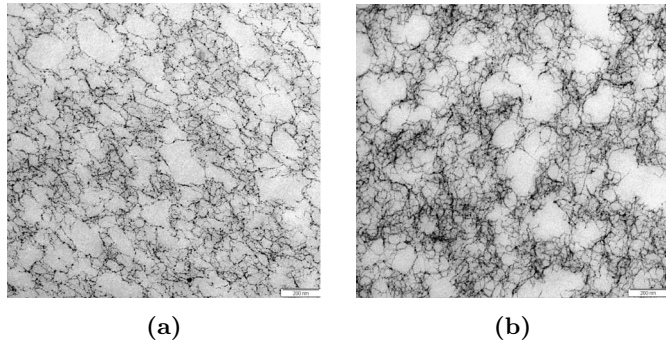


**Figure 4.3:** Comparison of internal (a) *vs.* external gelation method (b). TEM images of 60 nm thickness, the scale bar is 200 nm in both images (Paper I).

the two gelation mechanisms no visible difference in microstructure could be observed in the TEM images, which were taken in the bulk network, away from the vicinity of capillaries.

In general alginate capillary gels prepared by external gelation showed suitable mechanical properties to be used as a model system for characterising capillary flow. However, due to the high number of capillaries, it was difficult focussing on a single capillary and measure the speed of the meniscus, alginate gels made by internal gelation containing a single artificially created capillary was more suitable to study capillary flow in, which is described below.

### 4.3 LIQUID PENETRATION INTO AIR FILLED CAPILLARIES IN HYDROGELS

Agarose and alginate gels were produced in such a way that they contained an air filled capillary of micrometer size. The channel was connected to a liquid reservoir (droplet on a surface) and spontaneously the liquid penetrated the horizontal capillary. The travelled distance of the moving meniscus was recorded over time and an example is plotted in Fig. 4.4(a). The graph shows the squared travelled distance  $x^2$  of pure water over time in alginate gels with a capillary diameter of 180, 250, 410 and 630  $\mu\text{m}$ . The shaded areas represent the standard deviation of each time point ( $n \geq 5$ ). As can be seen, the lines in the graph follow the relation  $x^2 \propto t$  as predicted by Eq. (2.13). Only in the very early times at  $t < 0.25$  s, no linear relation can be observed, which

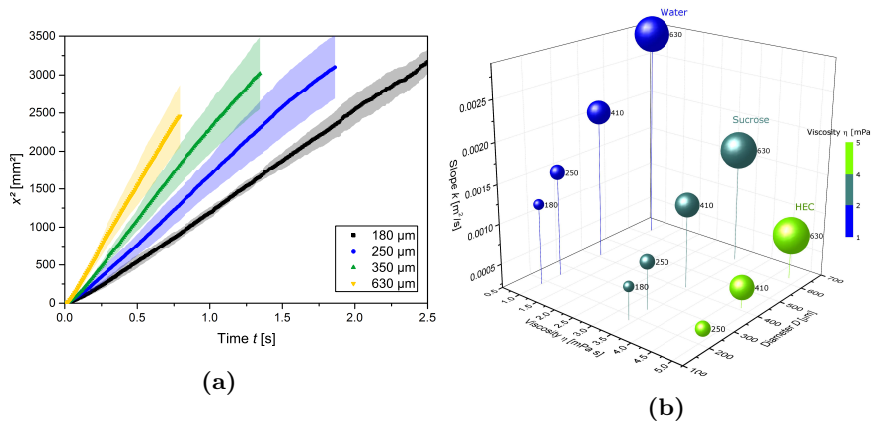


**Figure 4.4:** Liquid uptake in alginate capillaries of 180–630  $\mu\text{m}$  with (a) water, where the squared travelled distance over time is shown. (b) shows the slopes resulting from (a) for water and in addition a sucrose solution and a HEC solution over the viscosity and diameter of the capillary.

is likely to be an effect due to inertial forces. This relationship of  $x^2 \propto t$  is commonly found in various kinds of porous materials or single capillaries [9, 10, 13, 15]. Larger diameters result in faster capillary action, where the capillary having 630  $\mu\text{m}$  was already filled after 0.75 s, while it took in average 2.56 s for the capillary of 180  $\mu\text{m}$  to be completely filled with water. To be able to compare various results of different liquids and diameters, the slopes from the lines plotted in Fig. 4.4(a) were calculated starting from 50 % of the time to exclude inertial effects and assure a linear relationship.

Fig. 4.4(b) shows the slopes of three different liquids, namely pure water, a sucrose solution (21.4 % w/w) and a HEC solution (0.1 % w/w) in alginate gels. The slopes are plotted over the viscosity of the liquid and the capillary diameter, the latter is also indicated next to the balls in  $\mu\text{m}$  and by the scaled size of the balls. Out of the tested wetting liquids and diameters the channels of 630  $\mu\text{m}$  diameter were filled fastest with water, as the highest ball indicates. Having the highest viscosity out of the tested liquids, HEC resulted in the lowest slopes, specifically the smallest diameter tested, 250  $\mu\text{m}$ . The sucrose solution has slopes in between the ones of water and HEC as it has a viscosity in between those two. Thus, larger capillary diameter and lower viscosities result in faster capillary flow as it is predicted by Eq. (2.13).

Interestingly, if the slopes of our experiments in alginate, as well as in

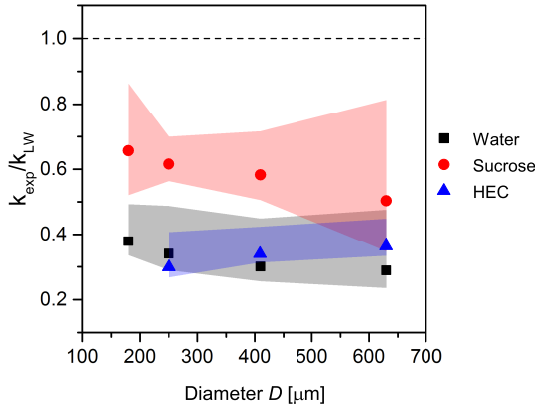


**Figure 4.5:** Ratio of the slopes of experimentaly determined values to Eq. (2.13) over the diameter  $D$  in alginate gels with the wetting liquids water (■), sucrose solution (●) and HEC solution (▲). The shaded areas represent the standard deviation and the dashed line LW behaviour.

agarose gels, are compared with the predictions of LW, large discrepancies are found. Fig. 4.5 shows how much the experiments deviate from the predictions. The ratio of the experimentally determined slopes  $k_{exp}$  to the slopes of Eq. (2.13)  $k_{LW}$  is plotted over the capillary diameter  $D$  in alginate capillaries and different wetting liquids, as indicated. The dashed line at  $k_{exp}/k_{LW}$  at 1 represents LW behaviour. As can be seen in the graph, water and HEC solution are only around 30–40 % as fast as the prediction by LW. This is the case for all tested diameters and a trend of the influence of diameters cannot clearly be identified, partly due to high standard deviations. The tests in agarose gels having a diameter of 250  $\mu\text{m}$  with water resulted in similar ratios. Sucrose solution in alginate gels appears closer to LW behaviour, but with relatively high standard deviations. Since the sucrose solution has a much higher concentration than the HEC solution, one can assume that an osmotic effect influences the flow, which besides other effects will be discussed in the section below.

#### 4.3.1 POSSIBLE REASONS FOR THE DEVIATION OF EXPERIMENT AND LW

INERTIAL EFFECTS are one common reason to address deviations to LW. Bosanquet [4] and Ridgway et al. [44] described the inertial flow regime before

viscous forces prevail, according to Eq. (2.16), which is valid for  $a \cdot t \ll 1$  (term  $a$  see (2.14)). The times for which the relationship  $a \cdot t \ll 1$  is valid can be calculated as

$$t \ll \frac{r^2 \rho}{8\eta}. \quad (4.1)$$

In the most critical case using water as wetting liquid having the lowest viscosity in the largest capillary of 630  $\mu\text{m}$  in diameter, inertial flow should be considered at  $t \ll 0.012$  s, equivalent to a distance of 1.6 mm away from the entrance. At this early time there are one or two measured time points in the experiments, with the majority being measured much later. The calculation of the slopes is, moreover, based on times starting from 50 % of the entire penetration time, which starts at 0.39 s for water in 630  $\mu\text{m}$ , equivalent to a distance of 35 mm from the entrance. Smaller diameters and higher densities (as in the case of sucrose) will still not change the threshold time to later times than the one mentioned. Therefore I conclude that inertial effects are not the reason for the deviation of the observed deviation from our experiments to LW.

DYNAMIC CONTACT ANGLE is another common reason to address deviations to LW since Eq. (2.13) is based on a static contact angle. Therefore I determined the contact angle directly in the capillary during the penetration process by analysing video images taken using an optical microscope. After  $\sim 2$  cm from the entrance contact angles of  $\sim 25^\circ$  were determined. Recalculating the predictions with contact angles which are achieved after 2 cm instead of the static contact angle, still resulted in large deviations to the experiments. It is concluded that the dynamic contact angle is not (solely) the cause for the large deviation to LW.

CHEMICAL POTENTIAL differences for water between the penetrated liquid and surrounding gel should be considered when concentration differences occur. However, conducting the same flow experiments having a calcium solution as the wetting liquid instead of water with the same ionic strength as the alginate gel gave no difference in speed of the meniscus. The sucrose solution in Fig. 4.5 shows slightly lower deviations to LW and one could assume that an osmotic effect is the reason for that. In that case water from the lower concentrated alginate gel would be drawn into the high concentrated sucrose solution leading to a thinning effect of the wetting liquid. The viscosity would decrease. Inserting lower  $\eta$  into Eq. (2.13) would lead to higher  $k_{LW}$ , the slope ratio would be lower and therefore closer to water and HEC solution.

---

### 4.3. LIQUID PENETRATION INTO AIR FILLED CAPILLARIES IN HYDROGELS

---

Thus, if the viscosity is lower in reality than expected due to osmotic effects, the prediction would deviate even more from the experiment.

INTERSTITIAL FLOW is reported to occur for both agarose [69] and alginate [70] upon forced water flow within gel capillaries. Interstitial flow occurs as the boundary layer of the flowing media ranges within the gel and not at the capillary gel interface, causing energy reduction. By calculating the total volumetric flow in the channel and the gel out of Stokes' and Brinkman's equation a correction term can be inserted into LW accounting for the permeable gel. However, with an expected permeability of the alginate, as well as the agarose gel, this effect of the loss of kinetic energy is too small to cause such a large deviation in penetration speed compared to the predictions (Tobias Gebäck, personal communication, March 7, 2016).

DEFORMATION of soft materials is the reason for slow spreading of droplets on flat surfaces [39]. A wetting ridge is formed at the three-phase contact line, described and pictured in section 2.1.2. It has been proposed that the deformation has consequences on the speed of a meniscus [20]. Accordingly not only viscous braking from Poiseuille flow has to be taken into account, but also braking due to viscoelastic forces of the substrate. The softer the material, the higher is the wetting ridge at the contact line and the slower the spreading. Shanahan and Carré [20] report a height of a wetting ridge of 60 nm with a silicone rubber having a Young's modulus of 1.9 MPa. As described in section 4.2, alginate gels produced by internal gelation resulted in a Young's modulus of 11 kPa. This agrees well with literature values where both an alginate gel of 2 % and an agarose gel of 1 % have Young's moduli of ~ 14 to 16 kPa [71]. Those values are much lower than the silicone rubber in [20]. It follows that an even higher wetting ridge could be formed in the alginate gels I used. Therefore I hypothesise that there is a wetting ridge occurring at the triple contact line of the moving meniscus in our experiments in alginate and agarose which slows down the meniscus due to the viscoelasticity of the gel. This is the object of further studies and will be tested experimentally.

## CHAPTER 5

# CONCLUSION AND FUTURE WORK

### 5.1 CONCLUSION

In this thesis I showed that it is possible to make use of capillary flow in gels containing predominantly water. One example of such a gel is an alginate gel, which can be produced in a certain way to contain straight and circular capillaries of tailored diameter. Finding a suitable model system to study the flow in, an alginate capillary gel produced via external gelation was compared to a gel fabricated by internal gelation. Mechanical characterisation of the two gels showed that internally set gels needed considerably more stress to maintain the gel at a given strain than the capillary gel and they ruptured later at higher stresses. Micrographs taken with TEM revealed pore sizes of maximum 200 nm but also more dense network. Aided by image analysis the mean pore diameter of a 60 nm thick slice was determined to  $\sim 60$  nm irrespective of the gel type. However, since the mechanical properties differed fundamentally, which could not solely be explained by the existence of capillaries, it suggests a structural difference of the two gels.

Using the alginate capillary gel as a model system to study capillary flow has shown to be unsuitable due to the high number of capillaries and the resulting difficulties to follow the meniscus in just one capillary. Therefore a method was developed to produce a single capillary of tailored size in a calcium-alginate gel produced by internal gelation. All water based test liquids completely penetrated the vertical  $\sim 6$  cm long capillaries with diameters of 180 to 630  $\mu\text{m}$  demonstrating that capillary action does occur in gel systems containing predominantly water. Thereby smaller diameters resulted in slower speeds and lower viscosities resulted in higher speeds, like Lucas [2] and Wash-

burn [3] predicted. The moving meniscus also followed the generally accepted and often cited general relationship of  $x^2 \propto t$ . Comparing absolute values of the slopes of  $x^2$  over  $t$  of prediction and experiment revealed large discrepancies. The experiments in the gels were only about one third of the prediction, irrespective of the diameter but with smaller difference for a sucrose solution. Since lower elastic modulus causes the spreading of a droplet on a surface to be significantly slowed down, it is hypothesised that deformation of the gel and with it the influence of elastic modulus causes the meniscus to be slowed down. The energy is therefore not only dissipated through the viscous flow, Poiseuille flow, but also by the viscoelasticity of the gel. This hypothesis needs further confirmation and is the subject of future investigations. Since it has been shown here that capillary flow does occur in porous gel systems, it is a promising method to disperse cells or solutes into the porous gel directly to achieve an even distribution of the desired substances and to simplify the process.

## 5.2 FUTURE WORK

The hypothesis that the viscoelastic deformation at the three-phase contact line of moving meniscus, gel wall and air causes the deviation of experiment and prediction of LW, needs to be confirmed and described mathematically. It could be tested by changing the elastic modulus of the gel and measure the travelled distance over time of a wetting liquid. Increased speed for higher moduli would be expected.

Moreover, the influence of the shape of the capillary wall on the travelled speed of a penetrating liquid is part of further studies. How do sharp edges versus soft edges influence the flow speed? An investigation of how the alginate gel wall looks like exactly would also be of use, especially to determine if it could have been damaged during fabrication of the channel.

After investigating the speed of a meniscus in single capillaries, it is also interesting to measure flow in porous systems like foams or paper and find relations to the results of the behaviour in single capillaries.

## ACKNOWLEDGEMENTS

I owe my deepest gratitude to my Anette Larsson, my main supervisor, who always knows how to motivate, speed up processes and has an ear for all other worries. It has been a pleasure to work with you and I hope of continued enjoyable work. I also share the credit of my work with Anna Ström, my co-supervisor, who was always there when I had any kind of questions. I adore your knowledge about polysaccharides, your presentation and communication skills and your excitement about gels. Your sometimes opposing opinion to Anette made me realize once more that science is not always black and white. I look forward to continue working with you. Thanks to Sven Engström for being a great examinor.

I also want to thank everybody in my project group of SuMo Biomaterials, who gave valuable comments, tips and suggestions for my project each time we met. And therewith, I am grateful for the financial support of SuMo Biomaterials to make this project possible.

I wish to thank Thomas Nann for the guidance while I was at Ian Wark in Adelaide, Australia, even though the results are not included in this thesis, I hope to use the knowledge in the future. I appreciated the clear, direct and logical way of working of you and tried to do so myself. Also the work of Karin Hedsten, who helped me a lot in the cleanroom at Chalmers and became my co-supervisor as well as Ulf Södervall who guided me through the cleanroom facilities is appreciated. I want to thank Mats Stading, who also is my supervisor and I hope we can work more together in the coming part of my PhD.

Thanks to everybody in my small group, especially Romain Bordes, who helped me a lot with contact angle and surface tension measurements and always had valuable input, Iina Solala, Linda Härdelin and former PhD students Sofie Gårdebjer and Anders Johnsson.

It has also been a pleasure to be part of the Dimond division with all people

involved – former and present – and I appreciate working together with you and all the *fika’s* we had.

Last but not least I want to thank my family, my wonderful and loving husband Daniel and our adorable daughter Lotta. You are the colours of my life and I am very lucky and happy to have you by my side.

# BIBLIOGRAPHY

- [1] de Gennes, P.-G., Brochard-Wyart, F. and Quéré, D., 2004. *Capillarity and wetting phenomena: drops, bubbles, pearls, waves.* Springer New York, New York, NY.
- [2] Lucas, R., 1918. Über das Zeitgesetz des kapillaren Aufstiegs von Flüssigkeiten. *Kolloid-Zeitschrift*, 23(1):15–22.
- [3] Washburn, E. W., 1921. The dynamics of capillary flow. *Physical Review*, 17(3):273–283.
- [4] Bosanquet, C., 1923. On the flow of liquids into capillary tubes. *Philosophical Magazine Series 6*, 45(267):525–531.
- [5] Masoodi, R. and Pillai, K. M., 2012. A general formula for capillary suction-pressure in porous media. *Journal of Porous Media*, 15(8).
- [6] Xiao, R., Enright, R. and Wang, E. N., 2010. Prediction and optimization of liquid propagation in micropillar arrays. *Langmuir*, 26(19):15070–15075.
- [7] Rawool, A. S., Mitra, S. K. and Kandlikar, S. G., 2005. Numerical simulation of flow through microchannels with designed roughness. *Microfluidics and Nanofluidics*, 2(3):215–221.
- [8] Kusumaatmaja, H., Pooley, C. M., Girardo, S., Pisignano, D. and Yeomans, J. M., 2008. Capillary filling in patterned channels. *Physical Review E*, 77(6):067301.
- [9] Fisher, L. R. and Lark, P. D., 1979. An experimental study of the washburn equation for liquid flow in very fine capillaries. *Journal of Colloid and Interface Science*, 69(3):486–492.

- 
- [10] Callegari, G., Tyomkin, I., Kornev, K. G., Neimark, A. V. and Hsieh, Y.-L., 2011. Absorption and transport properties of ultra-fine cellulose webs. *Journal of Colloid and Interface Science*, 353(1):290–293.
  - [11] Girardo, S., Palpacelli, S., De Maio, A., Cingolani, R., Succi, S. and Pisignano, D., 2012. Interplay between Shape and Roughness in Early-Stage Microcapillary Imbibition. *Langmuir*, 28(5):2596–2603.
  - [12] Rye, R. R., Yost, F. G. and O'Toole, E. J., 1998. Capillary Flow in Irregular Surface Grooves. *Langmuir*, 14(14):3937–3943.
  - [13] Yang, D., Krasowska, M., Priest, C., Popescu, M. N. and Ralston, J., 2011. Dynamics of capillary-driven flow in open microchannels. *The Journal of Physical Chemistry C*, 115(38):18761–18769.
  - [14] Han, A., Mondin, G., Hegelbach, N. G., de Rooij, N. F. and Staufer, U., 2006. Filling kinetics of liquids in nanochannels as narrow as 27 nm by capillary force. *Journal of Colloid and Interface Science*, 293(1):151–157.
  - [15] Tas, N. R., Haneveld, J., Jansen, H. V., Elwenspoek, M. and van den Berg, A., 2004. Capillary filling speed of water in nanochannels. *Applied Physics Letters*, 85(15):3274–3276.
  - [16] Vo, T. Q., Barisik, M. and Kim, B., 2015. Near-surface viscosity effects on capillary rise of water in nanotubes. *Physical Review E*, 92(5):053009.
  - [17] Karpitschka, S., Das, S., van Gorcum, M., Perrin, H., Andreotti, B. and Snoeijer, J. H., 2015. Droplets move over viscoelastic substrates by surfing a ridge. *Nature Communications*, 6:7891.
  - [18] Park, S. J., Weon, B. M., Lee, J. S., Lee, J., Kim, J. and Je, J. H., 2014. Visualization of asymmetric wetting ridges on soft solids with X-ray microscopy. *Nature Communications*, 5:4369.
  - [19] Shanahan, M. E. R. and Carré, A., 1995. Viscoelastic dissipation in wetting and adhesion phenomena. *Langmuir*, 11(4):1396–1402.
  - [20] Shanahan, M. E. and Carré, A., 2002. Nanometric Solid Deformation of Soft Materials in Capillary Phenomena. In M. Rosoff, editor, *Nanosurface chemistry*, pages 289–313. Dekker, New York.
  - [21] Klose, F., 2016. *Skeletal Muscle Differentiation in 3D Capillary Gels - Development of a Novel Bioreactor*. Master's thesis, Chalmers University of Technology, Göteborg, Sweden.

## BIBLIOGRAPHY

---

- [22] Willenberg, B. J., 2005. *Modular Tissue Scaffolding Tools: A New Family of Self-assembled Biomaterials Derived from Copper-Capillary Alginate Gels.* Ph.D. thesis, University of Florida.
- [23] Batich, C. D., Willenberg, B., Hamazaki, T. and Terada, N., 2009. Alginate gel scaffold having a plurality of continuous parallel microtubular copper capillaries. Patent US7601525B2.
- [24] Pawar, K. C., 2011. *In vitro and in vivo characterization of alginate based anisotropic capillary hydrogels to guide directed axon regeneration.* Ph.D. thesis, University of Regensburg.
- [25] Garg, R. K., Rennert, R. C., Duscher, D., Sorkin, M., Kosaraju, R., Auerbach, L. J., Lennon, J., Chung, M. T., Paik, K., Nimpf, J., Rajadas, J., Longaker, M. T. and Gurtner, G. C., 2014. Capillary Force Seeding of Hydrogels for Adipose-Derived Stem Cell Delivery in Wounds. *Stem Cells Translational Medicine*, 3(9):1079–1089.
- [26] Thumbs, J. and Kohler, H.-H., 1996. Capillaries in alginate gel as an example of dissipative structure formation. *Chemical physics*, 208(1):9–24.
- [27] Holmberg, K., Jönsson, B., Kronberg, B. and Lindman, B., 2003. *Surfactants and polymers in aqueous solution.* Wiley, 2 edition.
- [28] Barnes, G. and Gentle, I., 2005. Capillarity and the mechanics of surfaces. In *Interfacial science*. Oxford University Press Oxford.
- [29] Nishino, T., Meguro, M., Nakamae, K., Matsushita, M. and Ueda, Y., 1999. The lowest surface free energy based on -CF<sub>3</sub> alignment. *Langmuir*, 15(13):4321–4323.
- [30] Gao, L. and McCarthy, T. J., 2006. Contact Angle Hysteresis Explained. *Langmuir*, 22(14):6234–6237.
- [31] Wenzel, R. N., 1936. Resistance of solid surfaces to wetting by water. *Industrial & Engineering Chemistry*, 28(8):988–994.
- [32] Bhushan, B., 2013. Solid Surface Characterization. In *Tribology in Practice Series : Introduction to Tribology*. Wiley, Somerset, GB.
- [33] Cerman, Z., Striffler, B. F. and Barthlott, W., 2009. Dry in the water: the superhydrophobic water fern *Salvinia* – a model for biomimetic surfaces.

- In P. D. S. N. Gorb, editor, *Functional Surfaces in Biology*, pages 97–111. Springer Netherlands.
- [34] Cassie, A. B. D. and Baxter, S., 1944. Wettability of porous surfaces. *Transactions of the Faraday Society*, 40:546–551.
  - [35] Choi, C.-H. and Kim, C.-J., 2006. Large Slip of Aqueous Liquid Flow over a Nanoengineered Superhydrophobic Surface. *Physical Review Letters*, 96(6):066001.
  - [36] Michielsen, S. and Lee, H. J., 2007. Design of a Superhydrophobic Surface Using Woven Structures. *Langmuir*, 23(11):6004–6010.
  - [37] Kajiya, T., Brunet, P., Royon, L., Daerr, A., Receveur, M. and Limat, L., 2014. A liquid contact line receding on a soft gel surface: dip-coating geometry investigation. *Soft Matter*, 10(44):8888–8895.
  - [38] Silva, J. E., Geryak, R., Loney, D. A., Kottke, P. A., Naik, R. R., Tsukruk, V. V. and Fedorov, A. G., 2015. Stick-slip water penetration into capillaries coated with swelling hydrogel. *Soft Matter*, 11(29):5933–5939.
  - [39] Carré, A., Gastel, J.-C. and Shanahan, M. E. R., 1996. Viscoelastic effects in the spreading of liquids. *Nature*, 379(6564):432–434.
  - [40] Shanahan, M. E. R. and Gennes, P. G. d., 1987. Equilibrium of the Triple Line Solid/Liquid/Fluid of a Sessile Drop. In K. W. Allen, editor, *Adhesion 11*, pages 71–81. Springer Netherlands. DOI: 10.1007/978-94-009-3433-7\_5.
  - [41] Miller, R., Fainerman, V. B. and Kovalchuk, V. I., 2006. Bubble and Drop Pressure Tensiometry. In *Encyclopedia of Surface and Colloid Science*, volume 8, pages 1026–1040. CRC Press, 2nd edition.
  - [42] Hamraoui, A., Thuresson, K., Nylander, T. and Yaminsky, V., 2000. Can a Dynamic Contact Angle Be Understood in Terms of a Friction Coefficient? *Journal of Colloid and Interface Science*, 226(2):199–204.
  - [43] Zhmud, B., Tiberg, F. and Hallstensson, K., 2000. Dynamics of Capillary Rise. *Journal of Colloid and Interface Science*, 228(2):263–269.
  - [44] Ridgway, C. J., Gane, P. A. and Schoelkopf, J., 2002. Effect of Capillary Element Aspect Ratio on the Dynamic Imbibition within Porous Networks. *Journal of Colloid and Interface Science*, 252(2):373–382.

## BIBLIOGRAPHY

---

- [45] Slaughter, B. V., Khurshid, S. S., Fisher, O. Z., Khademhosseini, A. and Peppas, N. A., 2009. Hydrogels in Regenerative Medicine. *Advanced Materials*, 21(32-33):3307–3329.
- [46] Hoffman, R. L., 1975. A study of the advancing interface. I. Interface shape in liquid—gas systems. *Journal of Colloid and Interface Science*, 50(2):228–241.
- [47] Ross-Murphy, S. B., 1995. Rheological characterisation of gels. *Journal of Texture Studies*, 26(4):391–400.
- [48] Hoffman, A. S., 2012. Hydrogels for biomedical applications. *Advanced Drug Delivery Reviews*, 64, Supplement:18–23.
- [49] Draget, K. I., Moe, S. T., Skjåk-Braek, G. and Smidsrød, O., 2006. Alginates. In *Food polysaccharides and their applications*, Food science and technology, pages 289–334. CRC/Taylor & Francis, Boca Raton, FL, 2nd edition.
- [50] Draget, K. I., 2009. Alginates. In G. O. Phillips and P. A. Williams, editors, *Handbook of Hydrocolloids*, Woodhead Publishing Series in Food Science, Technology and Nutrition, pages 807–828. Woodhead Publishing, 2nd edition.
- [51] Mitchell, J. R. and Blanshard, J. M. V., 1976. Rheological Properties of Alginate Gels. *Journal of Texture Studies*, 7(2):219–234.
- [52] Zhang, J., Daubert, C. R. and Foegeding, E. A., 2005. Fracture Analysis of Alginate Gels. *Journal of Food Science*, 70(7):e425–e431.
- [53] Zhang, J., Daubert, C. R. and Allen Foegeding, E., 2007. A proposed strain-hardening mechanism for alginate gels. *Journal of Food Engineering*, 80(1):157–165.
- [54] Grant, G. T., Morris, E. R., Rees, D. A., Smith, P. J. C. and Thom, D., 1973. Biological interactions between polysaccharides and divalent cations: The egg-box model. *FEBS Letters*, 32(1):195–198.
- [55] Treml, H. and Kohler, H.-H., 2000. Coupling of diffusion and reaction in the process of capillary formation in alginate gel. *Chemical Physics*, 252(1–2):199–208.

- [56] Despang, F., Börner, A., Dittrich, R., Tomandl, G., Pompe, W. and Gelinsky, M., 2005. Alginate/calcium phosphate scaffolds with oriented, tube-like pores. *Materialwissenschaft und Werkstofftechnik*, 36(12):761–767.
- [57] Caccavo, D., Ström, A., Larsson, A. and Lamberti, G., 2016. Modeling capillary formation in calcium and copper alginate gels. *Materials Science and Engineering: C*, 58:442–449.
- [58] Stanley, N. F., 2006. Agars. In *Food polysaccharides and their applications*, Food science and technology, pages 217–238. CRC/Taylor & Francis, Boca Raton, FL, 2nd edition.
- [59] Rinaudo, M., 2008. Main properties and current applications of some polysaccharides as biomaterials. *Polymer International*, 57(3):397–430.
- [60] Barrangou, L. M., Daubert, C. R. and Allen Foegeding, E., 2006. Textural properties of agarose gels. I. Rheological and fracture properties. *Food Hydrocolloids*, 20(2-3):184–195.
- [61] Serwer, P., 1983. Agarose gels: Properties and use for electrophoresis. *Electrophoresis*, 4(6):375–382.
- [62] Arnott, S., Fulmer, A., Scott, W. E., Dea, I. C. M., Moorhouse, R. and Rees, D. A., 1974. The agarose double helix and its function in agarose gel structure. *Journal of Molecular Biology*, 90(2):269–284.
- [63] Braudo, E. E., 1992. Mechanism of galactan gelation. *Food Hydrocolloids*, 6(1):25–43.
- [64] Phan-Thien, N., 2002. *Understanding Viscoelasticity*. Advanced Texts in Physics. Springer Berlin Heidelberg, Berlin, Heidelberg.
- [65] Vlachopoulos, J. and Polychronopoulos, N., 2011. Basic Concepts in Polymer Melt Rheology and Their Importance in Processing. In M. Kontopoulou, editor, *Applied polymer rheology: polymeric fluids with industrial applications*. John Wiley & Sons, Hoboken, US.
- [66] Thiele, H. and Hallich, K., 1957. Kapillarstrukturen in ionotropen Gelen. *Kolloid-Zeitschrift*, 151(1):1–12.
- [67] Löfgren, C., Guillotin, S. and Hermansson, A.-M., 2006. Microstructure and Kinetic Rheological Behavior of Amidated and Nonamidated LM Pectin Gels. *Biomacromolecules*, 7(1):114–121.

## BIBLIOGRAPHY

---

- [68] Hermansson, A.-M., 2008. Structuring Water by Gelation. In J. M. Aguilera and P. J. Lillford, editors, *Food Materials Science*, pages 255–280. Springer New York. DOI: 10.1007/978-0-387-71947-4\_13.
- [69] Chen, T., Buckley, M., Cohen, I., Bonassar, L. and Awad, H. A., 2012. Insights into interstitial flow, shear stress, and mass transport effects on ECM heterogeneity in bioreactor-cultivated engineered cartilage hydrogels. *Biomechanics and Modeling in Mechanobiology*, 11(5):689–702.
- [70] Schuster, E., Sott, K., Ström, A., Altskär, A., Smisdom, N., Gebäck, T., Lorén, N. and Hermansson, A.-M., 2016. Interplay between flow and diffusion in capillary alginate hydrogels. *Soft Matter*.
- [71] Ahearne, M., Yang, Y. and Liu, K. K., 2008. Mechanical characterisation of hydrogels for tissue engineering applications. *Topics in tissue Engineering*, 4(12):1–16.